

IDEA AND PERSPECTIVE

Elements of disease in a changing world: modelling feedbacks between infectious disease and ecosystems

Elizabeth T. Borer,^{1*} 
 Lale Asik,^{2,3} 
 Rebecca A. Everett,⁴ 
 Thijs Frenken,^{5,6} 
 Angelica L. Gonzalez,⁷ 
 Rachel E. Paseka,¹ 
 Angela Peace,² 
 Eric W. Seabloom,¹ 
 Alexander T. Strauss,^{1,8} 
 Dedmer B. Van de Waal⁵  and
 Lauren A. White⁹ 

Abstract

An overlooked effect of ecosystem eutrophication is the potential to alter disease dynamics in primary producers, inducing disease-mediated feedbacks that alter net primary productivity and elemental recycling. Models in disease ecology rarely track organisms past death, yet death from infection can alter important ecosystem processes including elemental recycling rates and nutrient supply to living hosts. In contrast, models in ecosystem ecology rarely track disease dynamics, yet elemental nutrient pools (e.g. nitrogen, phosphorus) can regulate important disease processes including pathogen reproduction and transmission. Thus, both disease and ecosystem ecology stand to grow as fields by exploring questions that arise at their intersection. However, we currently lack a framework explicitly linking these disciplines. We developed a stoichiometric model using elemental currencies to track primary producer biomass (carbon) in vegetation and soil pools, and to track prevalence and the basic reproduction number (R_0) of a directly transmitted pathogen. This model, parameterised for a deciduous forest, demonstrates that anthropogenic nutrient supply can interact with disease to qualitatively alter both ecosystem and disease dynamics. Using this element-focused approach, we identify knowledge gaps and generate predictions about the impact of anthropogenic nutrient supply rates on infectious disease and feedbacks to ecosystem carbon and nutrient cycling.

Keywords

Coupled element cycles, Droop model, feedback, infected, mineralisation, nitrogen, carbon, nutrient recycling, pathogen transmission, stoichiometric model, susceptible.

Ecology Letters (2021) 24: 6–19

INTRODUCTION

One of the greatest impacts of human activities on Earth is the steady increase in the emission and supply of biologically reactive elements, such as nitrogen (N) and phosphorus, to fuel society and our growing population (Steffen *et al.*, 2015). This rapidly changing environmental context is altering the diversity, composition and interactions among species in all of Earth's environments (Erisman *et al.*, 2013). However, an overlooked effect of elevated anthropogenic nutrient supply is the potential to alter disease through a variety of mechanisms including changes in pathogen reproduction and transmission, host physiology and fitness, and vector density (Borer *et al.*, 2016; Preston *et al.*, 2016). Importantly, these changes in disease could feed back to alter ecosystem processes, especially for autotroph hosts, including net primary productivity, elemental uptake and elemental recycling. Currently, models in disease ecology rarely track organisms past death, yet death

from infection can alter elemental recycling and nutrient supply to living hosts (Ruudij *et al.*, 2005; Suttle, 2007). Thus, both disease and ecosystem ecology stand to grow as fields by exploring questions that arise at their intersection, including disease impacts on the cycling of carbon (C) and elemental nutrients (Preston *et al.*, 2016; Fischhoff *et al.*, 2020; Paseka *et al.*, 2020), and the role of death and nutrient recycling in disease dynamics.

We currently lack a framework for predicting the breadth of ways that infectious disease could impact elemental fluxes and stocks and, conversely, the ways in which recycling of nutrients from dead hosts could alter disease dynamics in living hosts. We suggest that this impasse has occurred, in part, because these areas of inquiry have arisen from different intellectual lineages and as a result have focused on different currencies and response variables. In particular, disease ecology has its roots in population ecology with a focus on host health and epidemiology (May and Anderson, 1979); over the

¹Department of Ecology, Evolution, and Behavior, University of Minnesota, St. Paul, MN 55108, USA

²Department of Mathematics and Statistics, Texas Tech University, Lubbock, TX 79409, USA

³Department of Mathematics, Data Sciences and Statistics, University of The Incarnate World, San Antonio, TX 78209, USA

⁴Department of Mathematics and Statistics, Haverford College, Haverford, PA 19041, USA

⁵Netherlands Institute of Ecology (NIOO), Droevendaalsesteeg 10, Wageningen 6708 PB, Netherlands

⁶Great Lakes Institute for Environmental Research (GLIER), University of Windsor, Windsor, Ontario N9B 3P4, Canada

⁷Department of Biology & Center for Computational and Integrative Biology, Rutgers University, Camden, NJ 80102, USA

⁸University of Georgia, Odum School of Ecology, Athens, GA 30602, USA

⁹National Socio-Environmental Synthesis Center, Annapolis, MD 21401, USA

*Correspondence: E-mail: borer@umn.edu

past few decades it has grown to include community interactions in its modelling and predictions (Johnson *et al.*, 2015; Seabloom *et al.*, 2015). Focal response variables in this discipline include the prevalence and spread rate of infection through a population (or community) of hosts. In contrast, ecosystem ecology, with roots in geoscience, oceanography, limnology and biogeochemistry, has made enormous advances linking the flux of elements between biotic and abiotic forms, and has embraced the importance of environmental microbes in controlling elemental flux rates (Chapin *et al.*, 2011). Focal response variables in this discipline include the amount and flux rates of energy and elements, particularly elemental nutrients. However, while there has been isolated progress linking ecosystems and disease (Suttle, 2007; Borer *et al.*, 2016; Preston *et al.*, 2016; Fischhoff *et al.*, 2020), to date, the potential key role that microbial pathogens of living primary producers play in altering flux rates of C and nutrients has received little attention. Similarly, while the impacts of environmental change have received substantial attention in disease ecology, there has been little attention to the role of host death in recycling nutrients to living hosts.

Here, we integrate approaches from ecosystem and disease ecology to illustrate the potential large effects of nutrient influx and recycling on pools of C and the prevalence and spread of infectious disease. To enable this synthesis, we develop a model that draws from the lineages of both disease and ecosystem ecology and uses elements as a shared currency. In particular, we develop a single model that tracks organic and inorganic N and primary producer biomass (or C) in living vegetation as well as litter and soil, and tracks the transmission, prevalence (proportion of host population that is infected) and basic reproduction number (R_0 , the number of new infections arising from an initial infection) of a directly transmitted infectious disease. Using this model, we demonstrate that anthropogenic nutrient supply and recycling can interact with disease to substantially alter predictions for both ecosystem and disease outcomes. We use a stoichiometric framework that describes the balanced uptake and recycling of C and nutrients as they pass through biological systems (Sternner and Elser, 2002). This element-focused modelling approach opens the door for new insights into the impact of anthropogenic nutrient supply on infectious disease and subsequent feedbacks to ecosystem C and nutrient cycling.

AN INTEGRATED MODELLING APPROACH

In spite of the strong lineages of research in disease and ecosystem ecology, both of which embrace interactions between microbes and their resources, these independent research areas rarely learn from each other. One important barrier is the lack of a common currency: ecosystem ecology generally works in a currency of elements or energy, whereas disease ecology generally uses a currency of host individuals or populations. While tracking 'infected carbon' may be somewhat non-intuitive for disease ecologists for whom entire hosts are generally fully infected or not – and also somewhat non-intuitive for ecosystem ecologists for whom C is simply an element – this approach helps to bridge the gap between these disciplines. Although the assumptions within each discipline

are standard and therefore may seem intuitive, neither is completely accurate. For example, when a single leaf of a tree becomes infected, describing the whole tree as moving from 'susceptible' to 'infected' fails to capture organismal biology and mischaracterises some aspects of the impact or dynamics of infection (e.g. potentially overestimating spread rate). Similarly, the elemental uptake and content of infected tissues can differ from healthy tissues. Thus, ecosystem models that ignore the influence of infection dynamics on elemental uptake also may miss important elemental dynamics. Thus, by tracking susceptible primary producers and infection-induced changes in physiology, chemistry and mortality, and defining living primary producers (hosts) in units of C and nutrients, we generate a model that captures the dynamics and feedbacks between disease and ecosystem characteristics.

Disease is well known for its impacts on mortality, but virulence also can lead to morbidity that alters physiological rates and elemental uptake and recycling in living hosts. For example, photosynthetic C capture rates have been shown to differ in infected and uninfected primary producers (Lobato *et al.*, 2010; Jiang *et al.*, 2016; Puxty *et al.*, 2016). Ecosystem studies tracking elements and energy may be reasonably accurate, without explicit attention to infection, because data are collected at large enough scales to average over infected and uninfected hosts. However, infection can scale up to induce substantial impacts at the ecosystem scale, leading to significantly reduced net primary production. For example, fungal infection can induce large reductions in biomass accumulation in forests and grasslands (Seabloom *et al.*, 2017; Fei *et al.*, 2019). These effects are not likely to remain constant with global change; increasing elemental nutrient supply to ecosystems (Steffen *et al.*, 2015), for example, can lead to increasing, decreasing or nonlinear changes in infection severity, pathogen spread and host mortality in plants (Dordas, 2008; Fones and Gurr, 2017; Paseka *et al.*, 2020). These impacts of infection can persist beyond host death as legacy effects of disease by inducing changes in plant nutrient and defensive chemistry that either speed up or slow down nutrient recycling (Jackrel *et al.*, 2019; Pazianoto *et al.*, 2019). Thus, by acknowledging that functional differences between infected and uninfected hosts may alter content and fluxes of C and nutrients at the ecosystem scale, we can ask how these relationships may qualitatively alter predictions for infection prevalence in host populations and C and nutrient dynamics in ecosystems with increasing nutrient supply.

Model structure

We developed the stoichiometric Ecosystem-Disease (ED) model, to examine the dynamic consequences of infection in a primary producer and feedbacks through both disease and ecosystem characteristics (Fig. 1; Table 1). Key processes in the model can be interpreted through lenses of disease or ecosystem ecology; for example, growth and death rates [disease] are analogous to rates of photosynthesis and litter production [ecosystem] (Table 2). While a variety of modelling approaches incorporate coupled elemental cycles via organismal physiology (Rastetter, 2011), we chose to use a Droop model formulation (Droop, 1973) to allow for a flexible

stoichiometric balance in the uptake and decomposition of host C and nutrients. While originally developed for phytoplankton, Droop models have been applied to a wide range of autotrophs, including vascular plants (Sterner and Elser, 2002; Nifong *et al.*, 2014). With the Droop formulation, the host uptake rate of one elemental nutrient varies with the availability of the others. While the ED model formulation is general, we use a forest as our case study so that we can compare the dynamics to a well-studied ecosystem model (Multiple-Element-Limitation, MEL) that describes a deciduous forest (Rastetter and Shaver, 1992; Rastetter *et al.*, 1997). The ED model represents a simpler alternative (e.g. no threshold functions) and includes fewer parameters than the MEL model approach (Rastetter and Shaver, 1992; Rastetter *et al.*, 1997). Appendix S1A provides details on the ED model formulation. However, in spite of these structural differences, when parameterised for a forest (in the absence of disease) analogous to Rastetter *et al.* (1997), these models yield quantitatively similar equilibrium predictions (Table S1). By developing an analogous model with fewer parameters necessary to describe healthy forest dynamics, we are able to expand the ED model to track both susceptible and infected vegetation (nearly doubling the number of parameters).

The ED model is a system of ordinary differential equations that represent susceptible and infected vegetation and the flow of C and N (Table 1). Here we track C and N as they move through susceptible (S) and infected (I) hosts. Photosynthetic C uptake describes growth, which produces uninfected tissue (as carbon, S). Growth rates, which differ for susceptible and infected vegetation (subscripted *S* and *I* respectively), follow Droop dynamics (Droop, 1973), depending on a maximum growth rate (μ , μ) and vegetation nutrient to C ratios (Q_s , Q_I). Because plants require nutrients for growth, we describe this constraint with a minimum N:C ratio (q_s , q_I). Variables Q_s and Q_I model these dynamical N:C ratios, which can vary between the minima (q_s , q_I) and maxima (Q , Q). The differential equations for Q_s , Q_I include terms for N:C dilution due to vegetation growth. We model virulence by implementing a cost of infection, with lower maximum growth rates ($\mu < \mu$) and higher death rates ($\delta_I > \delta_S$) for infected than susceptible

hosts. We couple nutrients into the infection dynamics by assuming, as with vegetation growth, that transmission (β) increases and saturates with nutrient content of infected plants (increasing N:C), based on empirical evidence in a wide range of primary producers (e.g. Mitchell *et al.*, 2003; Smith, 2007; Cronin *et al.*, 2010; Cheng *et al.*, 2019). In particular, susceptible hosts become infected at a rate that depends on the N:C ratio of infected hosts following a Michaelis–Menten (also known as ‘Holling type II’ or ‘Monod’) equation (Table 1), where β is the maximum transmission rate and κ is the half saturation constant (Table 2). Transmission results in a flow of vegetation C and vegetation nutrients from susceptible to infected, $\beta(Q_I)$, shown as solid and dashed arrows in Fig. 1. Once vegetation becomes infected, we assume that the N:C ratio changes from Q_s to Q_I . The shift in stoichiometry is tracked by the third term in the differential equation describing Q_I (Table 1).

We assume that constant death rates (δ_S and δ_I) produce litter, releasing vegetation C and N into the soil (following Rastetter *et al.*, 1997). Variables D_S and D_I track soil organic C, and R_S and R_I track soil organic N from susceptible and infected vegetation respectively. We assume constant rates of loss of soil organic C, either to long-term storage or movement out of the system as, for example, CO_2 or dissolved organic C, given by ϵ_S and ϵ_I . We do not track atmospheric C after it is released from the detritus via microbial respiration; we leave this for future work. The net mineralisation rate, or transformation of soil organic N into plant-accessible inorganic N (N, Fig. 1), occurs at rate r .

Vegetation uptake of soil inorganic N increases with N following Michaelis–Menten kinetics (Table 1), with maximum uptake rate c_i and half saturation constant a_i , for $i = S, I$ (Table 2). Uptake also depends on vegetation N:C ratios; as Q_i approaches its maximum value, Q , the uptake rate decreases. Vegetation N:C ratios decrease due to growth dilution (Sterner and Elser, 2002). We note that although the model (and Q_i , in particular) is formulated in terms of N:C, we present results in the ratio of C:N (Q_i^{-1}), more common in ecosystem ecology.

Finally, we derived the number of new infections per initial infection in a completely susceptible host population, or the

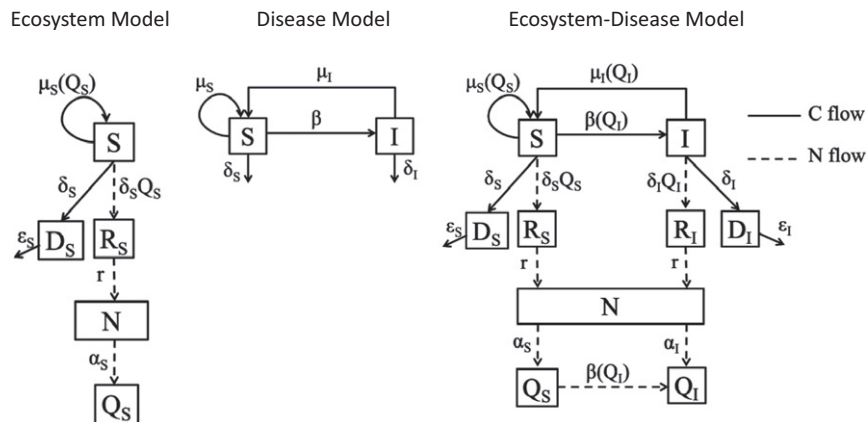


Figure 1 The Ecosystem-Disease (ED) model integrates key elements of ecosystem and disease ecology to track susceptible and infected hosts and the role of disease on pools and fluxes of elements as shown in Table 1.

Table 1 Model equations, state variables and units

$$\begin{aligned} \frac{dS}{dt} &= \underbrace{\mu_S(Q_S)S}_{\text{growth}} + \underbrace{\mu_I(Q_I)I}_{\text{infection}} - \underbrace{\beta(Q_I)SI}_{\text{infection}} - \underbrace{\delta_S S}_{\text{death}} \\ \frac{dI}{dt} &= \underbrace{\beta(Q_I)SI}_{\text{infection}} - \underbrace{\delta_I I}_{\text{death}} \\ \frac{dD_S}{dt} &= \underbrace{\delta_S S}_{\text{death released C}} - \underbrace{\varepsilon_S D_S}_{\text{C loss}} \\ \frac{dD_I}{dt} &= \underbrace{\delta_I I}_{\text{death released C}} - \underbrace{\varepsilon_I D_I}_{\text{C loss}} \\ \frac{dR_S}{dt} &= \underbrace{\delta_S S Q_S}_{\text{death released N}} - \underbrace{r R_S}_{\text{N recycling}} \\ \frac{dR_I}{dt} &= \underbrace{\delta_I I Q_I}_{\text{death released N}} - \underbrace{r R_I}_{\text{N recycling}} \\ \frac{dQ_S}{dt} &= \underbrace{\alpha_S(N, Q_S)}_{\text{N uptake}} - \underbrace{\mu_S(Q_S)Q_S}_{\text{growth dilution}} \\ \frac{dQ_I}{dt} &= \underbrace{\alpha_I(N, Q_I)}_{\text{N uptake}} - \underbrace{\mu_I(Q_I)Q_S}_{\text{growth dilution}} + \underbrace{\beta(Q_I)S[Q_S - Q_I]}_{\text{Infection induced change in N:C}} \\ \frac{dN}{dt} &= -\underbrace{\alpha_S(N, Q_S)S}_{\text{N uptake}} - \underbrace{\alpha_I(N, Q_I)I}_{\text{N uptake}} + \underbrace{r R_S + r R_I}_{\text{N recycling}} \end{aligned}$$

where

$$\text{Droop growth function: } \mu_i(Q_i) = \mu_i \left[1 - \frac{q_i}{Q_i} \right] \text{ for } i = S, I$$

$$\text{N uptake function: } \alpha_i(N, Q_i) = \frac{c_i N}{a_i + N} \left[\frac{Q_i - q_i}{Q_i - q_i} \right] \text{ for } i = S, I$$

$$\text{Transmission function: } \beta(Q_I) = \frac{\beta Q_I}{\kappa + Q_I}$$

Variable	Meaning	Units
S	Susceptible vegetation C	g C m^{-2}
I	Infected vegetation C	g C m^{-2}
D_S	Soil organic C from dead susceptible vegetation	g C m^{-2}
D_I	Soil organic C from dead infected vegetation	g C m^{-2}
R_S	Soil organic N from dead susceptible vegetation	g N m^{-2}
R_I	Soil organic N from dead infected vegetation	g N m^{-2}
Q_S	Susceptible host N:C ratio	gN gC^{-1}
Q_I	Infected host N:C ratio	gN gC^{-1}
N	Soil Inorganic N	g N m^{-2}

basic reproductive number (R_0) of the pathogen. Thus, the basic reproductive number depends on the disease-free equilibrium. It takes the following form:

$$R_0 = \frac{\beta(Q_I^*)S^*}{\delta_I} = \frac{\beta Q_I^* S^*}{(\kappa + Q_I^*) \delta_I}$$

where Q_I^* and S^* are the solutions for these state variables at the disease-free equilibrium. These values (Q_I^*, S^*) were obtained numerically using MATLAB ODE23 solver, with the initial condition $I_0 = 0$. Equilibria solutions were obtained after running the model long enough to ensure solutions were stabilised near steady-state values (10 000 years).

Model parameterisation

We parameterised this model using literature data from forest ecosystems to explore the consequences of anthropogenic N

supply for the dynamics of C, N and infection of forest vegetation. We examine the dynamics of a novel pathogen invading a forest (e.g. beech bark disease, sudden oak death, chestnut blight, Dutch elm disease, Fei *et al.*, 2019) by starting simulations with a very small amount of infected tissue (0.0005 of 22 000 g C m^{-2} in the forest, parameterised from Rastetter *et al.*, 1997).

While the ED model can be parameterised to describe infection in a wide range of primary producers (e.g. forest, lake, grassland), we take a 'modelling for understanding' approach (Rastetter, 2017) in which we use existing parameter ranges and recreate equilibria based on the extensive ecosystem modelling and empirical work that has been done in two deciduous hardwood forests (i.e. Harvard Forest and Hubbard Brook). Because forest ecosystem models typically do not include estimates for parameters associated with disease, we estimated parameter values for the ED model from a variety of sources (Table 2; for details of parameter estimation see Appendix S1B). Additionally, we performed a sensitivity analysis for this forest case study (Appendix S1C and Appendix S5) to determine the parameters for which estimation uncertainty would have the greatest impact if this model were to be used for prediction.

Here, we simulate the dynamics of this forest ecosystem to understand the dynamic consequences and magnitude of changes caused by disease relative to other ecosystem perturbations (e.g. doubling CO_2 , Rastetter *et al.*, 1997). Because trees are long-lived hosts, simulations to examine transient temporal dynamics were run for 1000 years; simulations to examine the sensitivity of equilibria to variation in disease and ecosystem parameters were run for 10 000 years. All model simulations take place in a closed ecosystem in which all N is recycled via, for example, mineralisation of soil organic N. In the current work, we examine the impacts of increasing N on ecosystem and disease dynamics by varying the total N among simulations. While a closed system is not an ecologically realistic scenario, we save simulations of an open system, in which N can be gained through processes such as N deposition and lost via processes such as leaching (Galloway *et al.*, 2008), for a future analysis. For simulation details, see Appendix S2.

RESULTS

While the ED model framework is general and could be parameterised to represent infection of primary producers in many different ecosystem types (e.g. grasslands, oceans, lakes), the parameterisation and simulations presented here describe a 350-year-old deciduous forest ecosystem with dynamics and equilibria in the absence of infection that have been described and analysed elsewhere (Appendix Table S1, Rastetter *et al.*, 1997). As in this previous work, we assume constant conditions (e.g. no phenological change or seasonal cycles). Thus, the patterns we describe provide qualitative insights into the influence of the feedbacks between elemental nutrient availability and disease dynamics.

Temporal dynamics and feedbacks

We examine the influence of disease and nutrient supply on the temporal dynamics and feedbacks within a forest

Table 2 Parameter names, meanings, values and units, when parameterised for a 350-year-old deciduous forest. For information about parameter estimation, see Appendix S1

Parameter	Meaning – ecosystem	Meaning – disease	Value
$\hat{\mu}_S$	Maximum photosynthetic rate of susceptible host vegetation	Maximum growth rate of susceptible host vegetation	0.0754 y^{-1}
$\hat{\mu}_I$	Maximum photosynthetic rate of infected host vegetation	Maximum growth rate of infected host vegetation	0.93 $\hat{\mu}_S \text{y}^{-1}$
q_S	Minimum whole plant N:C ratio of susceptible host vegetation	Susceptible host N:C ratio (minimum whole plant)	1/439 gN gC^{-1}
q_I	Minimum whole plant N:C ratio of infected host vegetation	Infected host N:C ratio (minimum whole plant)	1/439 gN gC^{-1}
c_S	Maximum N:C uptake rate of susceptible host vegetation	Susceptible host resource acquisition rate (maximum N:C)	$3.8 \times 10^{-4} \text{gN gC}^{-1} \text{y}^{-1}$
c_I	Maximum N:C uptake rate of infected host vegetation	Infected host resource acquisition rate (maximum N:C)	$1.001 * c_S \text{gN gC}^{-1} \text{y}^{-1}$
a_S	N:C uptake half saturation constant of susceptible vegetation	Resource acquisition (N:C) half saturation constant susceptible host veg	0.003 gN m^{-2}
a_I	N:C uptake half saturation constant of infected vegetation	Resource acquisition (N:C) half saturation constant infected host veg	0.003 gN m^{-2}
\hat{Q}_S	Maximum whole plant N:C of susceptible vegetation	Susceptible host chemistry (maximum N:C)	1/120 gN gC^{-1}
\hat{Q}_I	Maximum whole plant N:C of infected vegetation	Infected host chemistry (maximum N:C)	$1.25 * \hat{Q}_S \text{gN gC}^{-1}$
r	N mineralisation rate	Resource (N) supply (recycling) rate	0.0084 y^{-1}
β	Maximum transmission rate	Maximum transmission rate	$1.2 * 10^{-5} \text{m}^2 \text{gC}^{-1} \text{y}^{-1}$
κ	Transmission half saturation constant	Transmission half saturation constant	0.009 gN gC^{-1}
δ_S	Vegetation litter production rate of susceptible vegetation	Death rate of susceptible host vegetation	0.0412 y^{-1}
δ_I	Vegetation litter production rate of infected vegetation	Death rate of infected host vegetation	$1.001 * \delta_S \text{y}^{-1}$
ϵ_S	Microbial respiration and burial of susceptible vegetation carbon	Carbon loss rate of susceptible host vegetation	0.0648 y^{-1}
ϵ_I	Microbial respiration and burial of infected vegetation carbon	Carbon loss rate of infected host vegetation	$1.1 * \epsilon_S \text{y}^{-1}$

ecosystem by comparing cases when infection is or is not present. Simulations with disease begin with a very small amount of infection, and while spread is initially slow, infection eventually sweeps through the forest (Fig. 2a), with infection prevalence increasing to a final steady state after *c.* 400 years (Fig. 2b). Because of the rate of spread, the amount of infected vegetation increases rapidly between 200 and 400 years causing many disease and ecosystem properties to change rapidly in this 200-year period. The duration of the transient dynamics is surprisingly insensitive to the amount of C initially infected; even when the initial infection is 1000 times larger than shown in Fig. 2 ($I_0 = 0.5 \text{gC m}^{-2}$), the transient dynamics still last for 200 years (Appendix S2, Fig. 1).

In our simulation, feedbacks between infection prevalence, soil N, vegetation C and transmission play out over hundreds of years. Based on empirical evidence from many plant diseases, we assume that the maximum C:N is lower in infected than healthy vegetation (Mitchell *et al.*, 2003; Smith, 2007; Cronin *et al.*, 2010; LeRoy *et al.*, 2011). Because N is higher in infected vegetation, as infection sweeps through the forest, the model dynamics show a decline in the C:N of infected vegetation (Fig. 2c). Infected vegetation takes up N faster than uninfected vegetation (due to, e.g., physiological manipulation by the pathogen Monier *et al.*, 2017), so the spread of disease initially depletes soil inorganic N (Fig. 2f; ~year 200–300). Thus, overall forest growth is strongly N limited during this period. However, infected vegetation also has a slower maximum growth (i.e. photosynthetic) rate and an

elevated death (i.e. litter production) rate, which ultimately drives down vegetation C once infected hosts begin to die (Fig. 2e). Death of infected hosts releases soil inorganic N, causing it to build up in the system (Fig. 2f; ~year 300–700). Thus, in this closed system, soil inorganic N first decreases in the early stages of the epidemic, then increases as the epidemic progresses and hosts die, ultimately reaching a final, higher, steady state *c.* 600 years after the pathogen invades. Variation in vegetation C:N ratio throughout this period also drives complementary changes in transmission rate (β), a key disease parameter (Fig. 2d). Since we assume that transmission increases with N (declining C:N), transmission over time is inversely related to vegetation C:N. A surprising consequence is that *per capita* spread rate (i.e. transmission) is highest at the end of the epidemic (Fig. 2d), whereas population level spread is fastest in the middle (Fig. 2b; steepest increase after *c.* 300 years).

Ecosystem properties are significantly altered by feedbacks between disease and elemental nutrients. First, infection causes vegetation C to decline by 1kg m^{-2} when disease enters the system (Fig. 2e). For perspective, this decrease is twice the magnitude of change that is predicted when atmospheric CO_2 is doubled (Rastetter *et al.*, 1997). Thus, disease can drive meaningful changes in C storage. Soil C follows an almost identical trajectory (data not shown). As infection sweeps through the forest, soil N declines sharply (Fig. 2f; ~year 200–300) because of the higher N content (lower C:N) of infected vegetation. However, as vegetation mortality

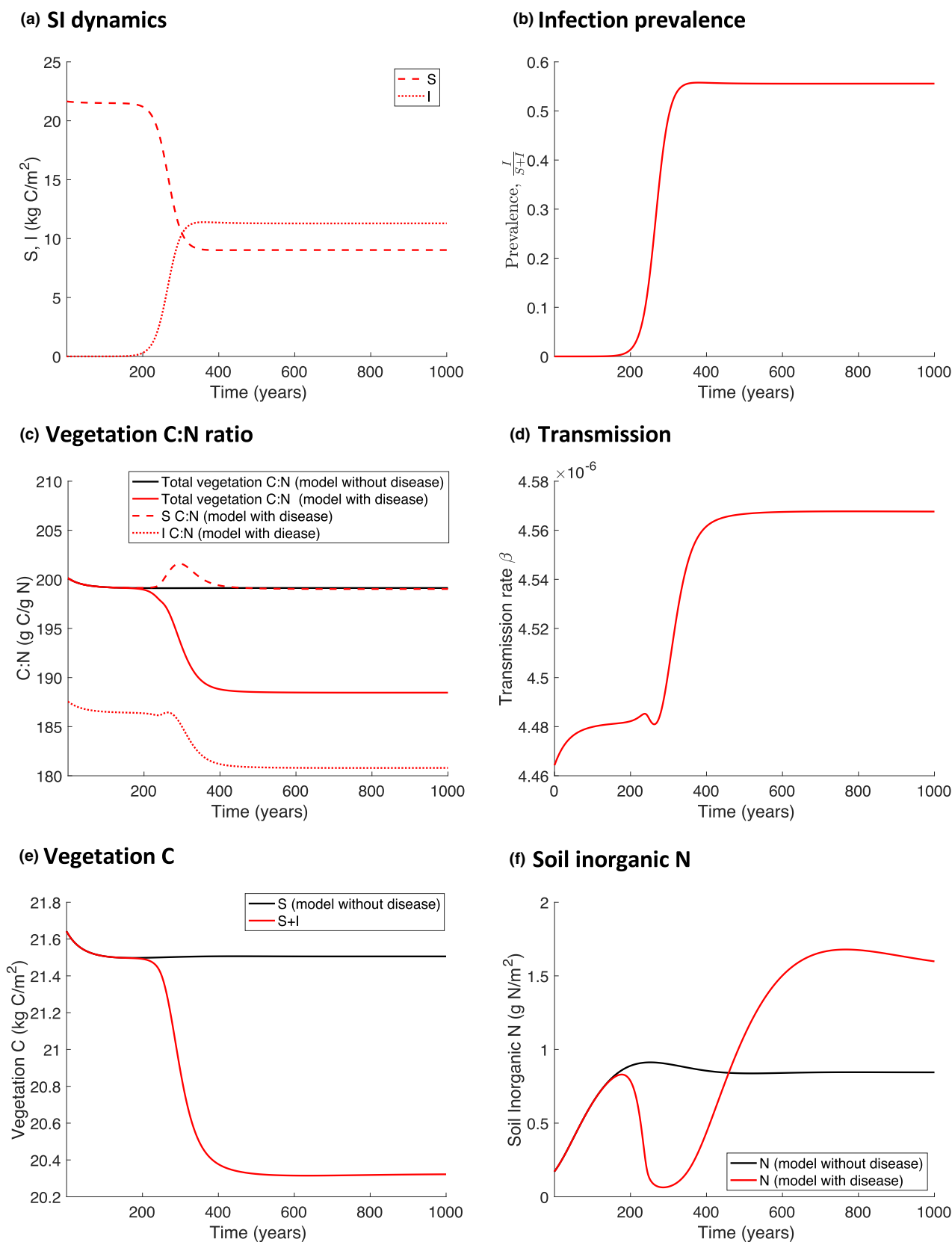


Figure 2 Predicted temporal dynamics of disease (panels a, b, d) and ecosystem (panels c, e, f) responses with the spread of infection of primary producers. Parameter values reflect a 350-year-old deciduous forest, with initial conditions and units shown in Table 1 with a small amount of initial infected vegetation; $S_0 = 2200$, $I_0 = 0.0005$, $D_{S0} = 1300$, $D_{I0} = 0$, $R_{S0} = 521$, $Q_{S0} = 190^{-1}$, $Q_{I0} = 190^{-1}$, $N_0 = 1$. In simulations without disease, $I_0 = 0$.

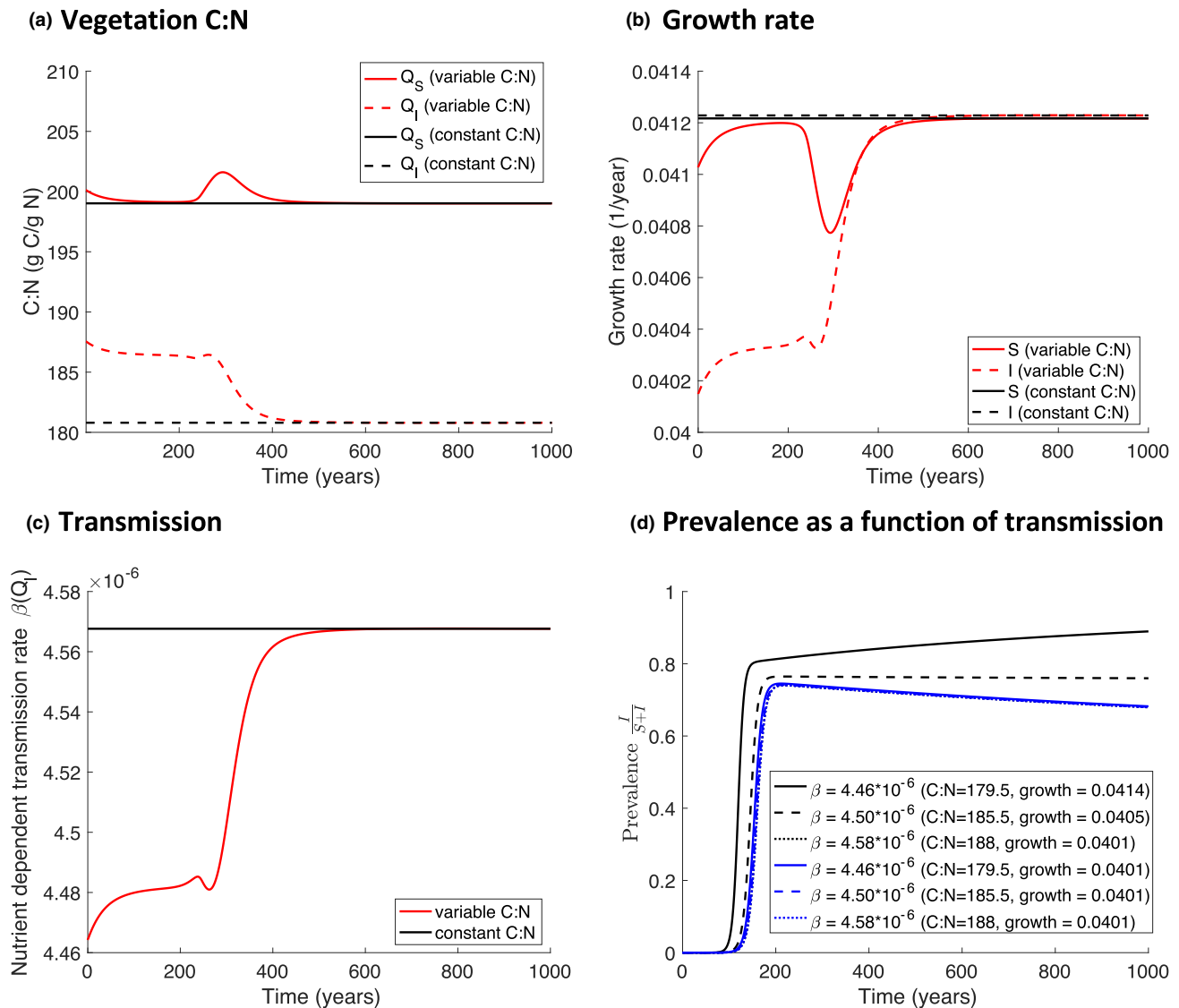


Figure 3 Transient dynamics of both ecosystem and disease properties are absent when infection is decoupled from nutrient dynamics (a–c, black lines, Appendix Table S2) compared to nutrient feedbacks to growth (a–c, red lines, Table 1). Feedbacks from infection to growth rates impact predictions for prevalence (d) across the range of transmission values shown in (c) in the constant C:N model. Panel (d) compares the constant C:N model with nutrient feedback to growth (black lines) and without feedback to growth (blue lines). Further details for the uncoupled case are in Appendix 2C and D.

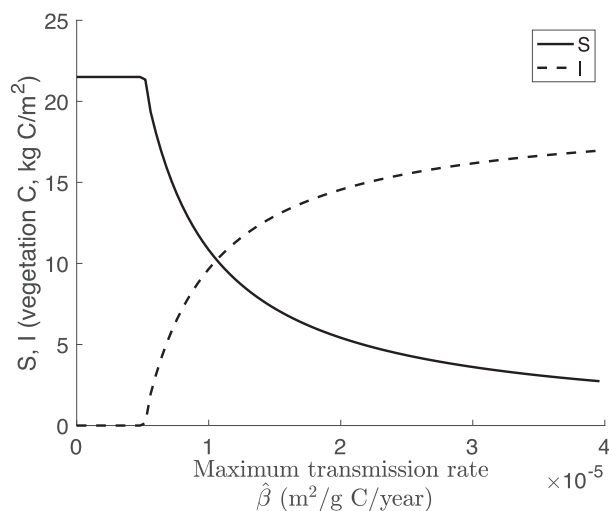
increases and total forest vegetation is reduced (Fig. 2e), there is a greater influx of N to the soil paired with reduced total uptake of N, leading to a slow (centuries long) approach of soil inorganic N to a new steady state that is nearly double that in a comparable forest without infection (Fig. 2f). Thus, disease can substantially alter predictions for both vegetation C and soil N over hundreds of years.

Importantly, these simulations demonstrate that the presence of infection and the feedbacks between disease and nutrient cycling lead to strong variation through time in both disease processes (e.g. transmission) and ecosystem properties (e.g. vegetation C, soil inorganic N). Non-intuitive outcomes arise, such as long-term fluctuations of soil inorganic N due to feedbacks among host elemental content, growth rate, transmission, death and decomposition as the pathogen spreads through the forest.

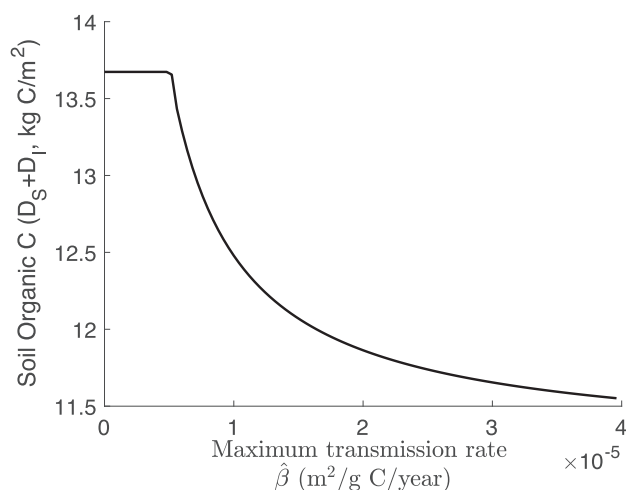
Feedbacks matter: interdependencies of plant chemistry and disease

Although most disease models assume no change in transmission as a function of environmental nutrient supply (but see Hurtado *et al.*, 2014), the results from our model suggest that the influence of ecosystem properties on temporal dynamics of infection may be strong. To examine the role of feedbacks between nutrient cycling and temporal disease and ecosystem dynamics, we simulated the forest ecosystem with and without feedbacks. In particular, we compared the system dynamics with and without coupling between disease and nutrient supply. We decoupled this ecosystem-disease linkage by assuming constant vegetation C:N ratios (hence constant transmission rates) set to match the final equilibrium values of the coupled simulations (equations in Appendix Table S2).

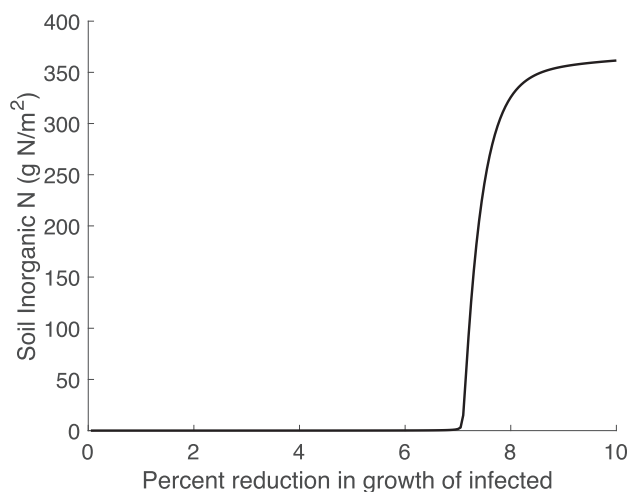
(a) Transmission and vegetation C



(b) Transmission and soil C



(c) Virulence and soil inorganic N



(d) Virulence and soil C

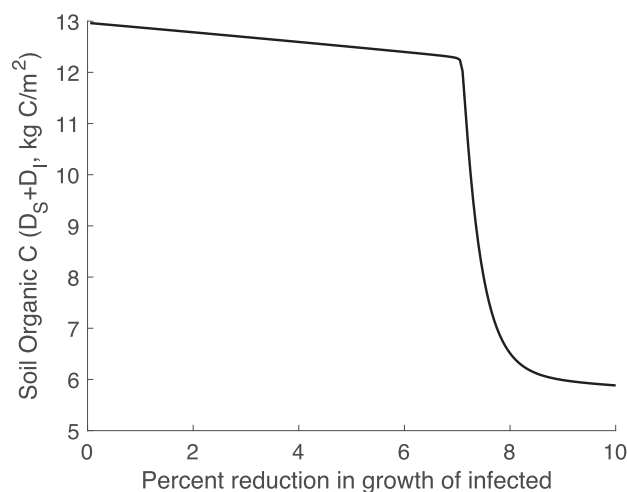


Figure 4 Impacts of disease properties, transmission (panels a, b) and virulence (panels c, d), on ecosystem, soil and vegetation, outcomes. Here, virulence in panels (c) and (d) is described as a percent reduction of the healthy vegetation photosynthetic (growth) rate ($\frac{\mu_t}{\mu_S} * 100$).

When nutrients can recycle and vary through time to influence pathogen transmission, long-term transient dynamics emerge (Fig. 3, red lines) that are not present in simpler disease models where resources are constant and decoupled from disease dynamics (Fig. 3, black lines). These transient dynamics can substantially alter ecosystem and disease predictions, including growth rates, vegetation chemistry and pathogen transmission for hundreds of years. For example, as infection spreads through the forest vegetation ($t = 200\text{--}400$ years), the growth (Fig. 3b) of infected vegetation is reduced because it is N limited (higher soil C:N due to reduced N, than at equilibrium, Fig. 3a). Even the growth rate of susceptible vegetation decreases – albeit less steeply – due to N limitation (solid red line; Fig. 3b), following the depletion of soil inorganic N (Fig. 2f). Transmission rate depends on the chemistry of the infected vegetation. Although transmission rate is reduced for hundreds of years as infection initially spreads through the forest, this rate accelerates as host death increases soil N. When modelled in a more traditional SI framework, these

dynamics are absent (Fig. 3, black lines). Thus, decoupling nutrient recycling from vegetation and disease dynamics, as in most disease models, generates substantially different long-term dynamics. Ignoring this coupling fails to capture long-term ecosystem-disease dynamics and feedbacks.

Notably, from a disease ecology perspective, transmission varies through time, responding to environmental nutrient supply (Fig. 3c). Across the range of transmission rates in Fig. 3c, when nutrient supply impacts transmission rates of the disease but also feeds back to alter growth rates of the host, this variation has a substantial impact on infection prevalence in the forest (Fig. 3d, black lines). However, when host growth rates do not vary with environmental nutrient supply (i.e. no ecosystem feedbacks) as in most disease model formulations, this same range of variation in transmission has virtually no impact on pathogen prevalence at the scale of the forest (Fig. 3d, blue lines; equations in Appendix Table S2). Thus, the coupling of disease with elemental supply and

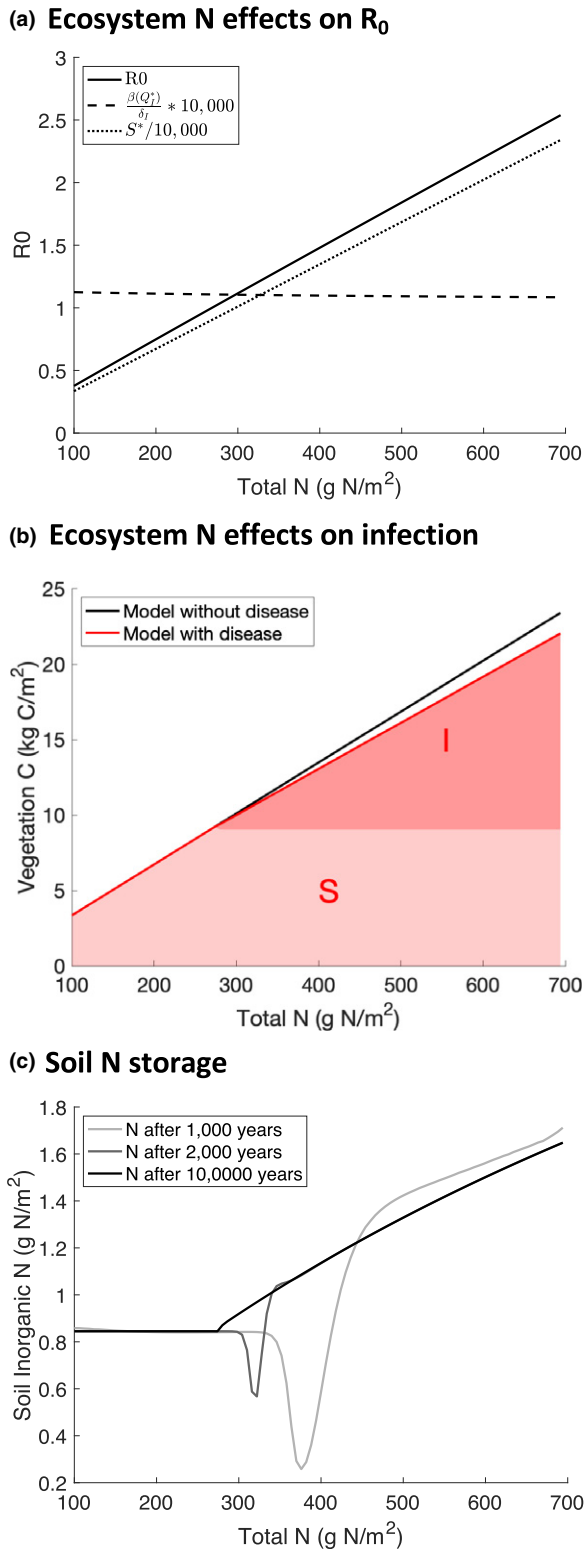


Figure 5 Contour figures depicting the response of disease dynamics and ecosystem properties to increasing total ecosystem N. Panel (a) shows the contribution of the two components of the R_0 equation to changes in ecosystem N; (b) shows the impact of disease on vegetation C; and (c) shows the long-term transient dynamics in soil N with increasing ecosystem N. The two components of R_0 (a) are changed by a factor of 10,000 for visualisation purposes, only (R_0 elasticity details presented in Appendix S4).

recycling leads to fundamentally different predictions for infection dynamics throughout the forest.

From an ecosystem perspective, the elemental composition (Fig. 3a) and the growth rate (Fig. 3b) of uninfected vegetation are impacted by the dynamic feedbacks induced by infection. These differences (Fig. 3a and 3b, dashed vs. solid lines) additionally demonstrate that the feedbacks via host death and nutrient recycling, that cause variation in transmission and growth rates, also determine long-term dynamics of the healthy (i.e. susceptible) vegetation.

Disease effects on long-term steady-state ecosystem properties

We examined the sensitivity of ecosystem properties of the forest to the rates of disease transmission and virulence. Unsurprisingly, we found a minimum transmission rate below which infection cannot persist in the forest (Fig. 4a). When this transmission rate is exceeded, infected vegetation biomass (as C) increases steadily with increasing transmission rate, replacing healthy vegetation. Because infected vegetation has a lower growth rate and higher death rate, once infection can be sustained in the forest, total vegetation declines, resulting in reduced long-term C storage in the forest soils (Fig. 4b). This transmission rate threshold corresponds with a bifurcation where the disease-free equilibrium and an endemic equilibrium exchange stability and the basic reproductive number passes the value of 1.

With increasing virulence of the pathogen (i.e. a greater disease-induced reduction in growth rate), total vegetation C and vegetation C:N decline. These dynamics lead to a buildup of inorganic N in the soil (Fig. 4c) and a decline in soil C (Fig. 4d). While inorganic N is soluble and the majority would likely be released from a forest with high infection (Rhoades *et al.*, 2017), the closed N cycle provides insight into the amount lost from the vegetation with increasing pathogen virulence.

When virulence reduces maximum growth rates, a threshold occurs where there is a sharp increase in soil inorganic N and a reduction in soil C (Fig. 4c & 4d, at approximately 7% growth rate reduction). While this abrupt threshold looks like a bifurcation (similar to 4a and 4b) we found no evidence for a bifurcation in this case (details in Appendix S3). Near this abrupt threshold, model predictions are extremely sensitive to small variations of this parameter, where vegetation density is more strongly influenced by changes in virulence, yielding rapid changes to soil N and C (see Appendix Fig. S2).

Ecosystem effects on long-term steady-state disease properties and feedbacks

We also examined the sensitivity of both disease and ecosystem properties to the total amount of N in the forest. At low ecosystem N, the number of new infections per initially infected host (R_0) is too low to sustain infection in the forest. With additional N, R_0 passes the critical threshold to sustain infection, and the pathogen can successfully invade and spread (Fig. 5a). This initial rate of spread increases with total ecosystem N, which, for the current parameter values, acts primarily as a function of the susceptible host equilibrium (dotted line in Fig. 5a), rather than changes in transmission rate (dashed line). More details on the elasticity of R_0 for

these factors are provided in Appendix S4. Total vegetation C (Fig. 5b) increases steadily with increasing ecosystem N. However, at low ecosystem N, the uptake and growth of healthy hosts is limited by N availability and infection cannot persist. When there is sufficient ecosystem N for the pathogen to invade, additional N leads to an increasing infection prevalence, an increasing proportion of forest C that is infected, and a slightly reduced amount of total vegetation C (Fig. 5b).

With sufficient N for infection to be sustained in the forest (approximately 270 g m^{-2} , where $R_0 > 1$), infected hosts take up and store N in their vegetation, causing soil inorganic N to decline (Fig. 5c). Surprisingly, at intermediate ecosystem N, infection feeds back to reduce soil N, in spite of increased N availability. This occurs because infected vegetation has higher N uptake (e.g. Fig. 2c), but most of the vegetation remains uninfected with this amount of ecosystem N (Fig. 5b), so soil inorganic N is drawn down but death rates are not substantially elevated. Although this reduction in soil inorganic N is transient, it takes thousands of years to shift from the vegetation to the soil at these intermediate rates of ecosystem N. Thus, while transient, the timescale of this shift is far longer than any empirical study, so likely represents a relevant biological outcome. With increased ecosystem N, the total ecosystem N availability is greater than the biological demand for growth, so soil inorganic N steadily increases with supply (Fig. 5c).

DISCUSSION

The ED model we present here builds a much-needed bridge between the fields of disease ecology and ecosystem ecology, and demonstrates the rich array of new dynamics that can arise and new questions that can be asked at this intersection. Explicitly including stoichiometric constraints on elemental uptake and the impacts of disease opens the door to a mechanistic understanding of the role of disease on nutrient limitation of growth and other biological process rates and elemental pools. Dynamic feedbacks between elemental nutrients and disease expand the range of questions about infectious disease to include relationships among nutrient supply, transmission, growth rates and virulence, infection prevalence, vegetation chemistry, nutrient recycling, and soil N and C storage. Thus, this single modelling framework allows us to examine disease impacts on ecosystem C and N pools and rates and, concurrently, track dead organisms that alter the nutrition of living hosts. With this framework, we can integrate the fields of ecosystem and disease ecology to gain a deeper understanding of the feedback loops that link them.

An important first step for determining whether including disease or disease-induced feedbacks alters ecosystem dynamics was to assess the impact of infection on the dynamics of a well-studied system. The MEL model (Rastetter and Shaver, 1992; Rastetter *et al.*, 1997), a mechanistic, multi-element model of a forest ecosystem provided just such an opportunity. This model has been used to study the short- and long-term impacts of a substantial ecosystem perturbation – an instantaneous doubling of atmospheric CO_2 – allowing us to contextualise the impact of disease. This exercise demonstrated that, for example, infection induced a decline in vegetation C that was nearly twice the magnitude of change induced by doubling CO_2 (Rastetter *et al.*,

1997). Similarly, in the final years of our simulations, infection in the forest caused an increase in soil inorganic N that was approximately double the magnitude predicted with a doubling of atmospheric CO_2 (Rastetter *et al.*, 1997). Thus, although our modelling goal was understanding and logical prediction, not forecasting (Mayr, 1998; Rastetter, 2017), comparing to a well-studied, mechanistic ecosystem model clarifies that disease sweeping through a forest may cause changes in ecosystem properties and feedbacks that are comparable to those of an extreme perturbation to elemental supply rates, providing critical context for this work. Importantly, these dynamics are supported by empirical data demonstrating that many widespread, non-native diseases of trees can cause substantial mortality (e.g. chestnut blight, Dutch elm disease, beech bark disease, dogwood anthracnose), leading to estimates of more than 3 Tg forest C lost each year in the United States to disease, alone (Fei *et al.*, 2019). Thus, these changes radically alter the cycling of forest C, and presumably other elements, as well. This modelling framework provides an opportunity for building our understanding of the feedbacks and outcomes of pathogen invasion for ecosystem dynamics.

Including biological realism in the form of coupled elemental resource uptake (Elser *et al.*, 2010) and a dependence of growth and infection on environmental nutrient supply (Bawden and Kassanis, 1950; Elser, 2006; Fatima and Senthil-Kumar, 2015) gave rise to a range of predictions for altered dynamics, feedbacks and legacy effects of pathogens in ecosystems. For example, the ED model, parameterised for a forest, predicted that disease would lead to an initial decline, then dramatic increase in soil inorganic N, due to short-term uptake followed by long-term feedbacks due to enriched vegetation N (reduced C:N). It also predicted, more rapid mineralisation, but ultimately reduced tree growth (photosynthetic rate) and uptake of N in a forest with disease. The ED model further demonstrated that increased pathogen transmission reduced forest vegetation C uptake, causing a decline in soil C storage. Empirical evidence tracking pathogen impacts is consistent with many of these predictions. For example, oomycete infection can change the chemistry of living host biomass in European beech trees (Wang *et al.*, 2003; Fleischmann *et al.*, 2004), even increasing N content and reducing C:N of litterfall in some tree species (Cobb *et al.*, 2013), with impacts on the rates of both nutrient uptake and litter decomposition and recycling (Cobb and Rizzo, 2016). Consistent with the ED model predictions, oomycete infection can reduce the photosynthetic rate (Fleischmann *et al.*, 2002), varying as a function of environmental nutrient supply (Fleischmann *et al.*, 2010). Empirical support for ED model dynamics is found in other ecosystems, as well. For example, in a mesocosm study, phytoplankton infection by chytrids (fungal parasites) suppressed the spring phytoplankton bloom, reduced biomass and reduced the C nutrient (elevated P content, in this case) in the seston (Frenken *et al.*, 2016; Frenken *et al.*, 2017). Viral infection in picocyanobacteria, the dominant primary producers in the oceans (Field *et al.*, 1998; Flombaum *et al.*, 2013), reduces photosynthetic rates (Puxty *et al.*, 2016). As a consequence, less C is fixed, causing a decline in the oceanic C sink. Estimates based on laboratory experiments, range from 0.02 up to 5.39 Pg C per year lost to viral-induced inhibition of CO_2 fixation, where the upper value approximates twice the net C uptake of the global oceans over 2000–2012 (Puxty *et al.*, 2016; Bindoff *et al.*, 2019).

While no studies quantifying the ecosystem impacts of forest pathogens map directly onto the scenario described in the ED model, the qualitative model predictions are surprisingly concordant with other, related, work in forests. For example, mortality of centuries-old forests from insect outbreaks can cause leaching and export of up to nearly 75% of the inorganic N (Rhoades *et al.*, 2017), qualitatively reflecting the ED model predictions for soil inorganic N release due to pathogen-induced mortality. In a temperate forest in which disease caused replacement of a dominant species (beech) by a new, N-rich species (sugar maple), analogous to disease altering the elemental content of the forest in the single-species ED model, the forest-scale ecosystem dynamics were remarkably similar to ED model dynamics. In particular, beech bark infection (bark-cankering fungus of the genus *Neonectria*) swept through New England forests in the 1950s causing beech mortality and replacement with sugar maple, and leading to increased forest-scale foliar N, soil inorganic N and decreased soil C:N (Lovett *et al.*, 2010), albeit via disease-induced species replacement rather than physiological changes in C and N dynamics with infection. Nonetheless, the qualitative predictions that emerge from tree–pathogen interactions in the parameterised ED model are borne out in these related scenarios.

The dependence of infection and growth on nutrient supply also led to feedbacks that substantially altered predictions of disease dynamics. The biologically motivated coupling of growth rates (Lobato *et al.*, 2010; Jiang *et al.*, 2016; Puxty *et al.*, 2016) and transmission rates (Smith, 2007; Fatima and Senthil-Kumar, 2015) to nutrient supply, although rarely included in models of disease dynamics (but see Hurtado *et al.*, 2014), led to feedbacks that accelerated *per capita* transmission rates through the epidemic and dramatically increased the predicted infection prevalence. When transmission was not coupled with growth rates, nutrient-induced changes in transmission caused virtually no change in infection prevalence. In disease ecology, there is an increasing recognition that the abstract concept of the transmission rate, β , is a representation that may overlook nonlinearities and heterogeneities in many host pathogen systems (McCallum *et al.*, 2017). For example, variation in transmission rate can be driven by variability in host contact behaviour, host physiology or infection-driven feedbacks on host behaviour (Ezenwa *et al.*, 2016; VanderWaal and Ezenwa, 2016; White *et al.*, 2018). While host immune responses as a function of resource availability have been considered (Cressler, Nelson, Day, & Mccauley, 2014), their connection to nutrient cycling processes that could drive transient dynamics in transmission rate at the ecosystem level remain unclear. Thus, variation in both growth and transmission rate with the nutrient environment, which can both change as a function of host mortality and affect host mortality in turn, points to an exciting avenue of inquiry by disease ecologists.

Disease and ecosystem ecology often function on very different timescales, but this model clarifies that disease may modify long-term forest dynamics in ways that change how we think about the system (Hastings, 2016). The timescales of decades, centuries and even longer that are predicted by this model may be inconceivably long for many disease ecologists, whereas these timescales are likely more familiar for ecosystem ecologists (Rastetter and Shaver, 1992; Rastetter *et al.*, 1997). These long

timescales in the current work arise primarily as a result of the relatively slow C uptake rates. Nonetheless, the model produced predictions that reflect timescales consistent with the documented rates of change in forest soils (Perruchoud *et al.*, 1999), including long-term soil responses to elevated tree mortality (due to, e.g., fire, logging, Bowd *et al.*, 2019). These results also suggest that in a younger forest (<140 yo), the dynamics and feedbacks in response to disease would likely operate significantly faster because of the relatively higher C uptake rates (Pugh *et al.*, 2019). While further model testing would benefit from experimentation in another ecosystem dominated by autotrophs with shorter generation times and rapid recycling rates (e.g. aquatic phytoplankton, Carpenter *et al.*, 1992), long-term data sets from ecosystems in which disease was monitored also could provide a valuable resource for further work (Knapp *et al.*, 2012). Given the long time lags from disease spread to ecosystem feedbacks, a model such as this one could be a strong candidate to provide early warning of long-term changes in elemental dynamics due to forest disease emergence (O'Regan and Drake, 2013).

While the ED model provides an important starting point for examining the intersection of disease and ecosystem dynamics, including other biologically realistic details, while outside the scope of the current work, will likely modify the predicted dynamics and lead to additional insights. For example, defensive compounds accumulated in response to infection while alive may substantially alter decomposition and nutrient recycling rates (Rahman *et al.*, 2013). At the scale of the forest, the ED model effectively described only a single species with 'trait' variation induced only by infection, yet inclusion of trait variation among individuals and species can alter dynamic predictions about ecosystem processes (Cianciaruso *et al.*, 2009). This form of realism could be particularly influential if, for example, transmission differed by species and the relative abundance of species changed in response to infection. Further, in the current formulation, we made the simplifying assumption that C was gained and lost (open system for C), but N was not (closed system for N), but a more realistic system with substantial N inputs and losses (Galloway *et al.*, 2008) could alter the fluxes and feedbacks of both C and N, as it did for a forest ecosystem without disease (Rastetter and Shaver, 1992; Rastetter *et al.*, 1997). The current model analysis suggests that additional biological realism that introduces heterogeneity in the host (e.g. stage- or age-structure) or in the infection processes (e.g. adding a recovered class) also could feed back to alter ecosystem processes. Finally, seasonality can influence disease in many systems (Altizer *et al.*, 2006), and if seasonal shedding of infected leaves reduces pathogen spread to uninfected host tissues or new hosts (Patharkar *et al.*, 2017), this could reduce pathogen spread and dramatically slow or alter the long-term feedbacks that influence nutrient recycling. These points each represent examples of the exciting range of questions that could build from the current model, informing the conditions under which disease will most strongly influence ecosystem dynamics.

Given the increasing rate of anthropogenic nutrient supply and the growing evidence of the importance of elemental nutrients in controlling the rates and impacts of infection in primary producers, exploring ecosystem consequences of

elemental nutrient supply is clearly important at the socio-environmental frontier for a variety of reasons. First, disease ecology has a multi-decadal history of delving into the effects of elemental nutrients in increasing infection virulence in hosts as well as the role of disease in controlling the relative competitive abilities of hosts and the resulting dynamics of host communities. However, the consequences of these nutrient–disease–host interactions for elemental pools and fluxes remain relatively unexplored (Mitchell, 2003; Preston *et al.*, 2016) even though these interactions modify key regulating ecosystem services. In contrast, ecosystem ecology has a strong focus on environmental microbes (e.g. bacteria and fungi involved in decomposition or N mineralisation); yet our growing awareness of the impacts of disease in living primary producers suggests that incorporating microbial infection in the living hosts (e.g. allocation of C or nutrients to growth vs defence, reduced photosynthetic rates, or increased respiration or mortality) could substantially alter our predictions for C and nutrient fluxes and the ecosystem services they underlie. The unified framework presented here provides a mechanism for explicit integration of the fields of disease and ecosystem ecology, opening the door to new questions and insights into the interplay of disease dynamics, ecosystem processes and changing biogeochemical cycles.

ACKNOWLEDGEMENTS

This work was supported by a grant to ETB from the National Socio-Environmental Synthesis Center (SESYNC) under funding received from the National Science Foundation DBI-1639145.

AUTHORSHIP

ETB and EWS conceived the idea; RAE, AP and ETB conceived the model structure with input from all others, and LA, RAE and AP developed and analysed the model; ETB wrote the paper and all the others contributed to writing.

DATA AVAILABILITY STATEMENT

The model code for equations and parameters, as well as code to reproduce figure 2 of this study, are openly available in Dryad at <https://doi.org/10.5061/dryad.0rxwdbxk>.

REFERENCES

Altizer, S., Dobson, A., Hosseini, P., Hudson, P., Pascual, M. & Rohani, P. (2006). Seasonality and the dynamics of infectious diseases. *Ecol. Lett.*, 9, 467–484.

Bawden, F.C. & Kassanis, B. (1950). Some effects of host nutrition on the susceptibility of plants to infection by certain viruses. *Annals of Applied Biology*, 37, 46–57.

Bindoff, N.L., Cheung, W.W.L., Kairo, J.G., Arístegui, J., Guinder, V.A.R. & Hallberg, N.H. *et al.* (2019). Changing Ocean, Marine Ecosystems, and Dependent Communities. In: *IPCC, 2019: IPCC Special Report on the Ocean and Cryosphere in a Changing Climate* (eds Pörtner, H.-O., Roberts, D.C., Masson-Delmotte, V., Zhai, P., Tignor, M. & Poloczanska, E. *et al* Intergovernmental Panel on Climate Change (IPCC). 447–588. <https://www.ipcc.ch/srocc/download/>

Borer, E., Laine, A.-L. & Seabloom, E. (2016). A multiscale approach to plant disease using the metacommunity concept. *Annu. Rev. Phytopathol.*, 54, 397–418.

Bowd, E.J., Banks, S.C., Strong, C.L. & Lindenmayer, D.B. (2019). Long-term impacts of wildfire and logging on forest soils. *Nat. Geosci.*, 12, 113–118.

Carpenter, S.R., Cottingham, K.L. & Schindler, D.E. (1992). Biotic feedbacks in lake phosphorus cycles. *Trends Ecol. Evol.*, 7, 332–336.

Chapin, F.S., Matson, P.A. & Vitousek, P.M. (2011). *Principles of Terrestrial Ecosystem Ecology*, 2nd edn. Springer, New York, NY.

Cheng, K., Frenken, T., Brussaard, C.P.D. & Van de Waal, D.B. (2019). Cyanophage propagation in the freshwater cyanobacterium *Phormidium* is constrained by phosphorus limitation and enhanced by elevated pCO₂. *Front. Microbiol.*, 10, 617. <https://doi.org/10.3389/fmicb.2019.00617>

Cianciaruso, M.V., Batalha, M.A., Gaston, K.J. & Petchey, O.L. (2009). Including intraspecific variability in functional diversity. *Ecology*, 90, 81–89.

Cobb, R.C., Eviner, V.T. & Rizzo, D.M. (2013). Mortality and community changes drive sudden oak death impacts on litterfall and soil nitrogen cycling. *New Phytol.*, 200, 422–431.

Cobb, R.C. & Rizzo, D.M. (2016). Litter chemistry, community shift, and non-additive effects drive litter decomposition changes following invasion by a generalist pathogen. *Ecosystems*, 19, 1478–1490.

Cronin, J.P., Welsh, M.E., Dekkers, M.G., Abercrombie, S.T. & Mitchell, C.E. (2010). Host physiological phenotype explains pathogen reservoir potential. *Ecol. Lett.*, 13, 1221–1232.

Dordas, C. (2008). Role of nutrients in controlling plant diseases in sustainable agriculture. A review. *Agron. Sustain. Dev.*, 28, 33–46.

Droop, M.R. (1973). Some thoughts on nutrient limitation in algae. *J. Phycol.*, 9, 264–272.

Elser, J. (2006). Biological stoichiometry: A chemical bridge between ecosystem ecology and evolutionary biology. *Am. Nat.*, 168, S25–S35.

Elser, J.J., Fagan, W.F., Kerkhoff, A.J., Swenson, N.G. & Enquist, B.J. (2010). Biological stoichiometry of plant production: metabolism, scaling and ecological response to global change. *New Phytol.*, 186, 593–608.

Erisman, J.W., Galloway, J.N., Seitzinger, S., Bleeker, A., Dise, N.B., Petrescu, A.M. *et al.* (2013). Consequences of human modification of the global nitrogen cycle. *Philos Trans R Soc Lond B Biol Sci*, 368, 20130116.

Ezenwa, V.O., Archie, E.A., Craft, M.E., Hawley, D.M., Martin, L.B., Moore, J. *et al.* (2016). Host behaviour - parasite feedback: an essential link between animal behaviour and disease ecology. *P Roy Soc B-Biol Sci*, 283.

Fatima, U. & Senthil-Kumar, M. (2015). Plant and pathogen nutrient acquisition strategies. *Frontiers. Plant Sci.*, 6, 750. <https://doi.org/10.3389/fpls.2015.00750>

Fei, S., Morin, R.S., Oswalt, C.M. & Liebhold, A.M. (2019). Biomass losses resulting from insect and disease invasions in US forests. *Proc. Natl Acad. Sci.*, 116, 17371.

Field, C.B., Behrenfeld, M.J., Randerson, J.T. & Falkowski, P. (1998). Primary production of the biosphere: Integrating terrestrial and oceanic components. *Science*, 281, 237–240.

Fischhoff, I.R., Huang, T., Hamilton, S.K., Han, B.A., LaDeau, S.L., Ostfeld, R.S. *et al.* (2020). Parasite and pathogen effects on ecosystem processes: A quantitative review. *Ecosphere*, 11, e03057.

Fleischmann, F., Göttelein, A., Rodenkirchen, H., Lütz, C. & Oßwald, W. (2004). Biomass, nutrient and pigment content of beech (*Fagus sylvatica*) saplings infected with *Phytophthora citricola*, *P. cambivora*, *P. pseudosyringae* and *P. undulata*. *Forest Pathol.*, 34, 79–92.

Fleischmann, F., Raidl, S. & Oßwald, W.F. (2010). Changes in susceptibility of beech (*Fagus sylvatica*) seedlings towards *Phytophthora citricola* under the influence of elevated atmospheric CO₂ and nitrogen fertilization. *Environ. Pollut.*, 158, 1051–1060.

Fleischmann, F., Schneider, D., Matyssek, R. & Oßwald, W.F. (2002). Investigations on net CO₂ assimilation, transpiration and root growth

- of *Fagus sylvatica* infested with four different *Phytophthora* species. *Plant Biology*, 4, 144–152.
- Flombaum, P., Gallegos, J.L., Gordillo, R.A., Rincón, J., Zabala, L.L., Jiao, N. *et al.* (2013). Present and future global distributions of the marine Cyanobacteria *Prochlorococcus* and *Synechococcus*. *Proc. Natl Acad. Sci.*, 110, 9824–9829.
- Fones, H.N. & Gurr, S.J. (2017). NOXious gases and the unpredictability of emerging plant pathogens under climate change. *BMC Biol.*, 15, 36.
- Frenken, T., Velthuis, M., de Senerpont Domis, L.N., Stephan, S., Aben, R., Kosten, S. *et al.* (2016). Warming accelerates termination of a phytoplankton spring bloom by fungal parasites. *Glob. Change Biol.*, 22, 299–309.
- Frenken, T., Wierenga, J., Gsell, A.S., van Donk, E. & Rohrlack, T. & Van de Waal, D.B. (2017). Changes in N:P supply ratios affect the ecological stoichiometry of a toxic cyanobacterium and its fungal parasite. *Front. Microbiol.*, 8, 1015. <https://doi.org/10.3389/fmicb.2017.01015>
- Galloway, J.N., Townsend, A.R., Erisman, J.W., Bekunda, M., Cai, Z.C., Freney, J.R. *et al.* (2008). Transformation of the nitrogen cycle: Recent trends, questions, and potential solutions. *Science*, 320, 889–892.
- Hastings, A. (2016). Timescales and the management of ecological systems. *Proc. Natl Acad. Sci.*, 113, 14568–14573.
- Hurtado, P.J., Hall, S.R. & Ellner, S.P. (2014). Infectious disease in consumer populations: dynamic consequences of resource-mediated transmission and infectiousness. *Theor. Ecol.*, 7, 163–179.
- Jackrel, S.L., Gilbert, J.A. & Wootton, J.T. (2019). The origin, succession, and predicted metabolism of bacterial communities associated with leaf decomposition. *MBio*, 10(5), e01703–01719.
- Jiang, Y., Ye, J., Veromann, L.-L. & Niinemets, Ü. (2016). Scaling of photosynthesis and constitutive and induced volatile emissions with severity of leaf infection by rust fungus (*Melampsora larici-populina*) in *Populus balsamifera* var. *suaveolens*. *Tree Physiol.*, 36, 856–872.
- Johnson, P.T.J., de Roode, J.C. & Fenton, A. (2015). Why infectious disease research needs community ecology. *Science*, 349, 1259504.
- Knapp, A.K., Smith, M.D., Hobbie, S.E., Collins, S.L., Fahey, T.J., Hansen, G.J.A. *et al.* (2012). Past, present, and future roles of long-term experiments in the LTER network. *Bioscience*, 62, 377–389.
- LeRoy, C.J., Fischer, D.G., Halstead, K., Pryor, M., Bailey, J.K. & Schweitzer, J.A. (2011). A fungal endophyte slows litter decomposition in streams. *Freshw. Biol.*, 56, 1426–1433.
- Lobato, A.K.S., Gonçalves-Vidigal, M.C., Vidigal Filho, P.S., Andrade, C.A.B., Kvitschal, M.V. & Bonato, C.M. (2010). Relationships between leaf pigments and photosynthesis in common bean plants infected by anthracnose. *New Zealand Journal of Crop and Horticultural Science*, 38, 29–37.
- Lovett, G.M., Arthur, M.A., Weathers, K.C. & Griffin, J.M. (2010). Long-term changes in forest carbon and nitrogen cycling caused by an introduced pest/pathogen complex. *Ecosystems*, 13, 1188–1200.
- May, R.M. & Anderson, R.M. (1979). Population biology of infectious diseases. 2. *Nature*, 280, 455–461.
- Mayr, E. (1998). *This is Biology: The Science of the Living World*. Belknap Press of Harvard University Press, Cambridge, MA.
- Mitchell, C.E. (2003). Trophic control of grassland production and biomass by pathogens. *Ecol. Lett.*, 6, 147–155.
- Mitchell, C.E., Reich, P.B., Tilman, D. & Groth, J.V. (2003). Effects of elevated CO₂, nitrogen deposition, and decreased species diversity on foliar fungal plant disease. *Glob. Change Biol.*, 9, 438–451.
- Monier, A., Chambouvet, A., Milner, D.S., Attah, V., Terrado, R., Lovejoy, C. *et al.* (2017). Host-derived viral transporter protein for nitrogen uptake in infected marine phytoplankton. *Proc. Natl Acad. Sci. USA*, 114, E7489–E7498.
- Nifong, R.L., Cohen, M.J. & Cropper, W.P. Jr (2014). Homeostasis and nutrient limitation of benthic autotrophs in natural chemostats. *Limnol. Oceanogr.*, 59, 2101–2111.
- O'Regan, S.M. & Drake, J.M. (2013). Theory of early warning signals of disease emergence and leading indicators of elimination. *Theor. Ecol.*, 6, 333–357.
- Paseka, R., White, L., Van de Waal, D.B., Strauss, A., González, A., Everett, R. *et al.* (2020). Disease-mediated ecosystem services: Pathogens, plants, and people. *Trends Ecol. Evol.*, 35, 731–743.
- Patharkar, O.R., Gassmann, W. & Walker, J.C. (2017). Leaf shedding as an anti-bacterial defense in *Arabidopsis* cauline leaves. *PLoS Genet.*, 13, e1007132.
- Pazianoto, L.H.R., Solla, A. & Ferreira, V. (2019). Leaf litter decomposition of sweet chestnut is affected more by oomycete infection of trees than by water temperature. *Fungal Ecol.*, 41, 269–278.
- Perruchoud, D., Joos, F., Fischlin, A., Hajdas, I. & Bonani, G. (1999). Evaluating timescales of carbon turnover in temperate forest soils with radiocarbon data. *Global Biogeochem. Cycles*, 13, 555–573.
- Preston, D.L., Mischler, J.A., Townsend, A.R. & Johnson, P.T.J. (2016). Disease ecology meets ecosystem science. *Ecosystems*, 19, 737–748.
- Pugh, T.A.M., Lindeskog, M., Smith, B., Poulter, B., Arneth, A., Haverd, V. *et al.* (2019). Role of forest regrowth in global carbon sink dynamics. *Proc. Natl Acad. Sci.*, 116, 4382–4387.
- Puxty, R.J., Millard, A.D., Evans, D.J. & Scanlan, D.J. (2016). Viruses inhibit CO₂ fixation in the most abundant Phototrophs on earth. *Curr. Biol.*, 26, 1585–1589.
- Rahman, M.M., Tsukamoto, J., Tokumoto, Y. & Shuvo, M.A.R. (2013). The role of quantitative traits of leaf litter on decomposition and nutrient cycling of the forest ecosystems. *Journal of Forest and Environmental Science*, 29, 38–48.
- Rastetter, E.B. (2011). Modeling coupled biogeochemical cycles. *Front. Ecol. Environ.*, 9, 68–73.
- Rastetter, E.B. (2017). Modeling for understanding v. modeling for numbers. *Ecosystems*, 20, 215–221.
- Rastetter, E.B., Agren, G.I. & Shaver, G.R. (1997). Responses of N-limited ecosystems to increased CO₂: a balanced-nutrition, coupled-element-cycles model. *Ecol. Appl.*, 7, 444–460.
- Rastetter, E.B. & Shaver, G.R. (1992). A Model of multiple-element limitation for acclimating vegetation. *Ecology*, 73, 1157–1174.
- Rhoades, C.C., Hubbard, R.M. & Elder, K. (2017). A Decade of streamwater nitrogen and forest dynamics after a mountain pine beetle outbreak at the Fraser experimental forest, Colorado. *Ecosystems*, 20, 380–392.
- Ruardij, P., Veldhuis, M.J.W. & Brussaard, C.P.D. (2005). Modeling the bloom dynamics of the polymorphic phytoplankter *Phaeocystis globosa*: impact of grazers and viruses. *Harmful Algae*, 4, 941–963.
- Seabloom, E.W., Borer, E.T., Gross, K., Kendig, A.E., Lacroix, C., Mitchell, C.E. *et al.* (2015). The community ecology of pathogens: coinfection, coexistence and community composition. *Ecol. Lett.*, 18, 401–415.
- Seabloom, E.W., Kinkel, L., Borer, E.T., Hautier, Y., Montgomery, R.A. & Tilman, D. (2017). Food webs obscure the strength of plant diversity effects on primary productivity. *Ecol. Lett.*, 20, 505–512.
- Smith, V. (2007). Host resource supplies influence the dynamics and outcome of infectious disease. *Integr. Comp. Biol.*, 47, 310–316.
- Steffen, W., Richardson, K., Rockström, J., Cornell, S.E., Fetzer, I., Bennett, E.M. *et al.* (2015). Planetary boundaries: Guiding human development on a changing planet. *Science*, 347(6223), 1259855.
- Sterner, R.W. & Elser, J.J. (2002). *Ecological Stoichiometry: The Biology of Elements from Molecules to The Biosphere*. Princeton University Press, Princeton, NJ.
- Suttle, C.A. (2007). Marine viruses — major players in the global ecosystem. *Nat. Rev. Microbiol.*, 5, 801–812.
- VanderWaal, K.L. & Ezenwa, V.O. (2016). Heterogeneity in pathogen transmission: mechanisms and methodology. *Funct. Ecol.*, 30, 1606–1622.
- Wang, Z.Y., Göttlein, A., Rodenkirchen, H., Fleischmann, F. & Oßwald, W. (2003). The influence of *Phytophthora citricola* on rhizosphere soil solution chemistry and the nutritional status of European beech seedlings. *J. Phytopathol.*, 151, 365–368.
- White, L.A., Forester, J.D. & Craft, M.E. (2018). Covariation between the physiological and behavioral components of pathogen transmission: host heterogeneity determines epidemic outcomes. *Oikos*, 127, 538–552.

SUPPORTING INFORMATION

Additional supporting information may be found online in the Supporting Information section at the end of the article.

Editor, John Drake

Manuscript received 3 June 2020

First decision made 15 July 2020

Manuscript accepted 1 September 2020